

Supplementary materials and methods

Immunohistochemistry and HE staining

Microarray development of human/mice tumors and single-staining were performed according to our previously described methods(1, 2). For human, anti-BAP1 (ab199396, Abcam,1:200) , anti-CCL2 (ab9669, Abcam,1:300) , anti-CCL3 (ab32609, Abcam,1:50) , anti-CCL4 (ab235961, Abcam,1:100), anti-CCL5 (ab9679, Abcam,1:150), anti-CCL8 (ab9671, Abcam,1:500) and anti-CCR5 (ab110103, Abcam,1:25) were used for staining. Human gastric cancer paraffin-embedded tissue microarrays were applied as positive controls and negative controls were achieved by replacing the staining antibodies with phosphate buffer saline. All reagents required in immunohistochemistry (IHC) were obtained from ZSGB-BIO. All slides were viewed with Leica DM6000 B (Leica Microsystems). IHC for BAP1, CCL2, CCL3, CCL4, CCL5, CCL8 and CCR5 expression in this study were all assessed by using a semi-quantitative H-score. The staining intensity was graded as 0 (negative), 1 (weak), 2 (moderate) and 3 (strong). The staining extent was scored as the percentage of positive cells or nucleus (0–100%). Both were multiplied to generate the semi-quantitative H-score, giving a range of 0–300. The staining intensity and extent were scored independently by two pathologists who were blind to the patients' characteristics. For all IHC quantitation, 3 randomly selected fields from 3 cross-sections of each tumor (i.e. 9 fields) were used to quantitate the percentage of tissue positive for each marker. The cutoff value for BAP1 and CCR5 were the median value. The cut-off points were set at 69.0 and 23.4, separately. Hematoxylin and eosin (HE) staining of mice tumor sections was performed according to the previous protocol(3).

Flow cytometry

Firstly, fresh tumor tissues were collected in DBSS (Gibco). The necrotic, fatty or normal sections were removed carefully. Then, tissues were cut into minor pieces and digested into single-cell suspension by using collagenase IV, hyaluronidase (Sigma Aldrich), 0.002% DNase I (Roche) and fetal bovine serum at room temperature for 3 hours. The staining procedure was followed by manufacturer's instructions (BD Biosciences) and our previous protocols (1). Especially, for intracellular cytokine measurements, the cells were stimulated for 5 hours with phorbol myristate acetate (50ng/ml) and ionomycin (1 µg/ml) in the presence of GolgiStop Protein Transport Inhibitor (1:1000).

Cells were examined by a FACSCelesta flow cytometer (BD Biosciences) and analyzed by FlowJo V10. For anti-human antibodies, anti-CD3 (SK7), anti-CD4 (RPA-T4), anti-CD25 (M-A251), anti-CD69 (FN50), anti-IFN-γ (B27), anti-CD8 (RPA-T8), anti-PRF1 (δG9), anti-CD107a (H4A3), anti-CD11c (B-ly6), anti-CD80 (L307.4), anti-CD326 (EBA-1), anti-CD45 (HI30), anti-CD127 (HIL-7R-M21) from BD Pharmingen and anti-Ki67 (Ki-67), anti-GZMB (GB11), anti-CD86 (BU63), anti-HLA-DR (L234), anti-PD-L1 (29E.2A3), anti-CCR5 (J418F1), anti-FOXP3 (206D) from Biolegend were used. For anti-mouse antibodies, anti-CD3 (17A2), anti-CD4 (RM4-5), anti-CD8 (53-6.7), anti-CD11c (HL3), anti-CD25 (PC61), anti-CD45 (30-F11), anti-IFN-γ (XMG1.2) from BD Pharmingen and anti-CCR5 (HM-CCR5), anti-GZMB (GB11), anti-PRF1 (S16009A), anti-CD80 (16-10A1), anti-CD86 (GL-1), anti-MHC-II (M5/114.15.2), anti-PD-L1 (10F.9G2), anti-PD-1 (29F.1A12), anti-CTLA4 (UC10-4B9), anti-FOXP3 (MF-14) from Biolegend were used.

Cell culture and in vitro therapeutic studies

As mentioned in our previous study (1), we cultured single-cell suspensions from human ccRCC tumors in vitro 3D assay medium (The DMEM/F12 medium prepared with 2% Matrigel (BD) and supplemented with 100 IU/mL rhIL-2 (R&D Systems), 50 U/mL rhGM-CSF (R&D Systems), 100 U/mL penicillin, 100 µg/mL streptomycin and 10% fetal bovine serum) for 12 hours at 37°C and 5% CO₂. Afterwards, cells were cultured with an isotype control antibody or a CCR5 antagonist (Maraviroc, Absin, abs810489) for four days. Cells were then collected via digestion by 0.1 U/mL Liberase DH (Roche) and subjected to phenotypic analysis by flow cytometry.

For measuring the dead tumor cells fraction after the treatment, Zombie Violet (Invitrogen, L34957), a Live/Dead Fixable Aqua Dead Cell Staining Kit for 405 nm excitation, was used as manufacturers' instruction. Dead cells were identified as populations that stained positive for the viability dye. Then we stained surface markers of tumor cells (CD45⁻Epcam⁺) for 30 minutes at 4°C in the dark and examined by a FACS Celesta flow cytometer (BD Biosciences) subsequently.

Isolation of PBMC-derived CCR5⁺ Tregs

Human peripheral blood from ccRCC patients was collected in anticoagulation tubes and subsequently used to isolate peripheral blood mononuclear cells (PBMCs) using Lymphoprep (Axis-Shield). To isolate PBMC-derived Tregs, T lymphocytes were first positively isolated by CD3-labeled magnetic beads (Miltenyi). Then lymphocytes were

stained at 10^6 cells/ml. CCR5⁺ Tregs used for cell sorting were defined as CD3⁺CD4⁺CD8⁻CD25⁺CD127⁻CCR5⁺. The sorted cells were used when their viability was determined > 90% and their purity was determined > 95%. After cell-surface staining for 20 minutes, CCR5⁺ and CCR5⁻ Tregs (CD3⁺CD4⁺CD8⁻CD25⁺CD127⁻) were subsequently sorted with the MoFlo XDP sorter (Beckman). Isolated PBMC-derived CCR5⁺ and CCR5⁻ Tregs was cultured in RPMI 1640 medium supplemented with a 1:40 dilution of ImmunoCult Human CD3/CD28/CD2 T Cell Activator (Stemcell Technologies) and 100 IU/mL rhIL-2 (R&D Systems) for related analysis.

Mice and in vivo studies

BALB/c mice were obtained from Charles River Laboratories (4-6 weeks old, female). RENCA (ATCC CRL-2947), a renal adenocarcinoma cell line originating from BALB/c mice were obtained from the Cell Bank of the Chinese Academy of Sciences. To knock down BAP1 in tumor cells, shBAP1 (ORIGENE TL513604V) lentiviral particles were used according to protocol. Scrambled shRNA (ORIGENE Cat#: TR30021V) was used as control.

All mouse experiments were approved by National Institutes of Health guidelines and institutional review board and ethics committee of Fudan University. The subcutaneous and orthotopic renal model were generated according to our preceding protocol(1). For BAP1 knock-down orthotopic renal model, mice were randomly grouped on day 14 based on body weight, injected with anti-CCR5 antibody (Creative Biolabs) systemically or isotype control antibody at a dose of 100 μ g twice weekly. Mice were sacrificed at about 4

weeks (39 days) post injection and then fresh tumor tissues were immediately evaluated by flow cytometry. For BAP1 knock-down subcutaneous renal model, mice were grouped on day 56 based on body weight, systemically injected with anti-CCR5 antibody or isotype control antibody with a dose of 100ug twice a week. Tumor volume were monitored every week using formula $V = 0.5 \times \text{length} \times \text{width}^2$, and mice were all sacrificed at the end of 16 weeks. For BAP1-wildtype orthotopic renal model, Mice were grouped on day 42 based on body weight and were all sacrificed at the end of 18 weeks. For BAP1-wildtype subcutaneous renal model, mice were grouped on day 70 based on body weight, systemically injected with anti-CCR5 antibody or isotype control antibody with a dose of 100ug twice a week. Tumor volume were monitored every week using formula $V = 0.5 \times \text{length} \times \text{width}^2$, and mice were all sacrificed at the end of 20 weeks.

BAP1 mutant analysis

For BAP1 mutant studies, tissue processing, nucleic acid extraction, primer design and sequencing were conducted as previously described (4). The BAP1 primer using for PCR amplification and sequences were performed(5): forward primer 5'-GCCTGCCTGACCATCACC and reverse primer 5'-AAGGAAAGCAGTAGGGAAGGA (Supplementary Figure 2d).

Migration assay

Chemotaxis was assayed using Falcon PET Cell Culture Inserts, 8- μm pore. CCL2, CCL3, CCL4, CCL5, CCL8 were used in migration assay, all from Absin. Isolated PBMC-derived

Tregs medium were seeded in the upper chamber at 1×10^5 in 0.5ml serum-free RPMI and 1ml of medium alone or supplemented with 100ng/ml recombinant chemokines with were added to lower chamber. Cells on the upper surface of the filter were removed by applicator carefully and migrated cells on the lower surface were stained with 0.1% Crystal Violet Staining Solution after overnight incubation at 37°C and 5% CO₂. For each insert, the number of migrated cells/field (40×) was evaluated.

Real-time PCR

Total RNA from human tumor specimens was extracted using TRIzol reagent (Invitrogen) according to manufacturers' instructions. Real-time quantitative PCR was performed on the Applied Biosystems 7300 Real-Time PCR system using SYBR Green dye (Applied Biosystems) as described by the manufacturer. The primers for CCL2 are as follows: 5': GATCTCAGTGCAGAGGCTCG and 3': TTTGCTTGTCCAGGTGGTCC; CCL3: 5': ATGGCTCTCTGCAACCAGTTCTC and 3': CCGGCTTCGCTTGGTTAGGA; CCL4: 5': GCTTCCTCGCAACTTTGTGG and 3': TCACTGGGATCAGCACAGAC; CCL5: 5': TGCTGCTTTGCCTACATTGC and 3': CTTGTTCAGCCGGGAGTCAT; CCL8: 5': TCCAGAGGCTGGAGAGCTACAC and 3': CCTGACCCATCTCTCCTTGGGG; CCR5: 5': ATCTGGCATAGTCTCATCTGGC and 3': GGCTGCGATTTGCTTCACAT. GAPDH served as an endogenous control. The $\Delta\Delta C_t$ method was applied to estimate relative transcript levels.

ELISA

The concentrations of CCL2-5, CCL8, IL-10 and TGF- β 1 were assessed (all from R&D Systems) according to the manufacturer's instructions. Human/mouse CCL2-5, CCL8 and human IL-10 and TGF- β 1 were assessed by ELISA Kits in supernatants of patient tumor tissue and RENCA cell lines. Also, Arginase Activity Colorimetric Assay Kit (BioVision) and Nitric Oxide Synthase (NOS) Activity Assay Kit (BioVision) were evaluated. Human IL-10 and TGF- β 1 were evaluated in supernatants of CCR5⁺ Tregs and CCR5⁻ Tregs from BAP1-mutant human peripheral blood. And similar experiments were used to test the pro-inflammatory cytokines production such as GM-CSF and TNF- α in gastric tumor tissue supernatants(6, 7)

Statistical analysis

Continuous variables between different groups were analyzed by t tests. Categorical variables were analyzed by Chi-square or Fisher's exact test. Multivariate analyses were used to determine the hazard ratios (HR, 95% confidence interval) of ccRCC patient characteristics (detailed in Supplementary Table 1). Survival analysis (OS and RFS) were assessed by Kaplan-Meier method and compared by the log rank test. The number of immune cells or functional molecules or genes compared two groups by using Student's t test or Mann-Whitney U test, compared two groups from the same patients by using paired t-test. Spearman's correlation test was used to evaluate the association between two genes. All grouped data in the figures was represented by the mean \pm SD with significance indicated (*, for $p < 0.05$, **, for $p < 0.01$, ***, for $p < 0.001$; ns, no significance). All tests were two-sided. The graphical and statistical analyses were performed using GraphPad Prism Software (version 7.00) and IBM SPSS Statistics software (Version 22).

References

1. Fu Q, Xu L, Wang Y, Jiang Q, Liu Z, Zhang J, et al. Tumor-associated macrophage-derived interleukin-23 interlinks kidney cancer glutamine addiction with immune evasion. *European urology*. 2019;75(5):752-63.
2. Liu Z, Zhu Y, Xu L, Zhang J, Xie H, Fu H, et al. Tumor stroma-infiltrating mast cells predict prognosis and adjuvant chemotherapeutic benefits in patients with muscle invasive bladder cancer. *Oncoimmunology*. 2018;7(9):e1474317.
3. Brugarolas J. Molecular genetics of clear-cell renal cell carcinoma. *Journal of clinical oncology*. 2014;32(18):1968.
4. Peña-Llopis S, Vega-Rubín-de-Celis S, Liao A, Leng N, Pavía-Jiménez A, Wang S, et al. BAP1 loss defines a new class of renal cell carcinoma. *Nature genetics*. 2012;44(7):751.
5. Farley MN, Schmidt LS, Mester JL, Pena-Llopis S, Pavia-Jimenez A, Christie A, et al. A novel germline mutation in BAP1 predisposes to familial clear-cell renal cell carcinoma. *Molecular cancer research*. 2013;11(9):1061-71.
6. Lv Y, Zhao Y, Wang X, Chen N, Mao F, Teng Y, et al. Increased intratumoral mast cells foster immune suppression and gastric cancer progression through TNF-alpha-PD-L1 pathway. *J Immunother Cancer*. 2019;7(1):54.
7. Wang T-t, Zhao Y-l, Peng L-s, Chen N, Chen W, Lv Y-p, et al. Tumour-activated neutrophils in gastric cancer foster immune suppression and disease progression through GM-CSF-PD-L1 pathway. *Gut*. 2017;66(11):1900-11.

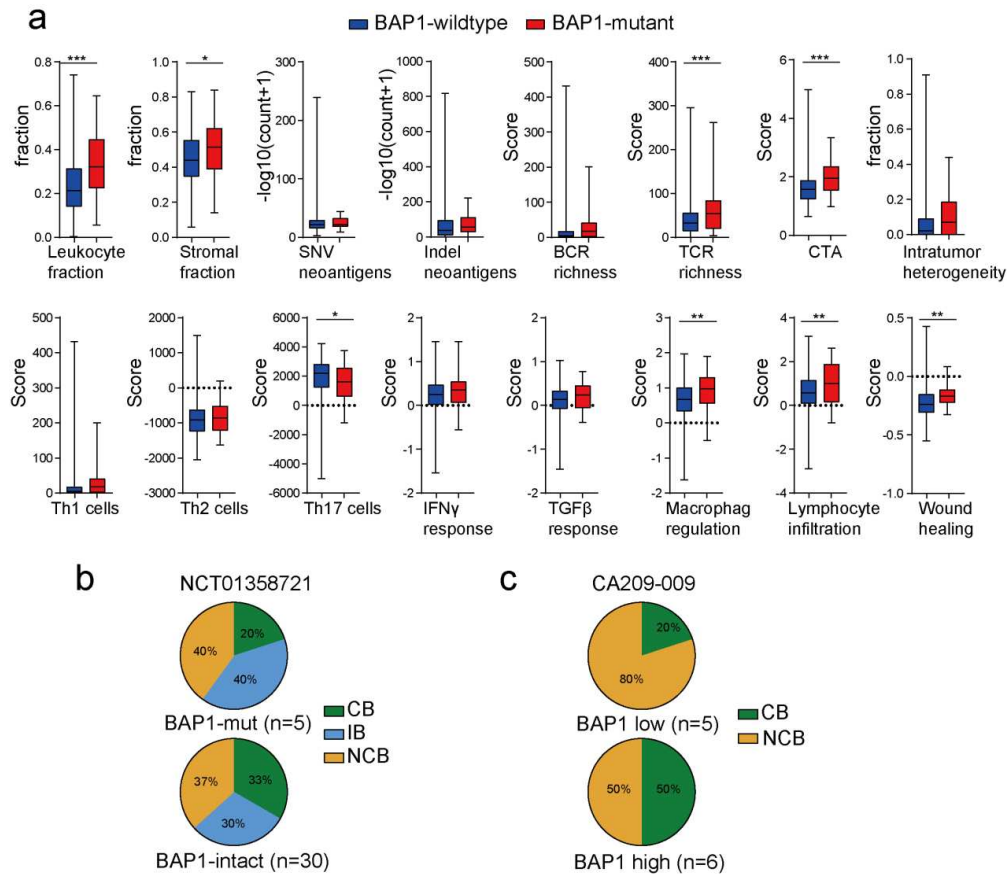
Supplementary Table 1. Patient characteristics

| Characteristic | TCGA cohort (n = 533) | Shanghai cohort (n = 797) |
|---|-----------------------|---------------------------|
| Age at surgery (years) | | |
| Median (quartile) | 61 (52 to 70) | 56 (47 to 63) |
| Gender | | |
| Male | 345 (65%) | 563 (70.6%) |
| Female | 187 (35%) | 234 (29.4%) |
| Unknown | 1 (0.2%) | 0 |
| ECOG-PS | | |
| 0 | 40 (7.5%) | 673 (84.4%) |
| ≥1 | 16 (3.0%) | 124 (15.6%) |
| Unknown | 477 (89.5%) | 0 (0%) |
| Surgery | | |
| Radical nephrectomy | 312 (58.5%) | 463 (58.1%) |
| Partial nephrectomy | 106 (19.9%) | 316 (39.6%) |
| Laparoscopic radical nephrectomy | 103 (9.3%) | 18 (2.3%) |
| Laparoscopic partial nephrectomy | 12 (2.3%) | 0 |
| Tumor size (cm) | | |
| Median (quartile) | 5.5 (3.7 to 8.5) | 3.5 (2.5 to 5.0) |
| Pathological T stage (categorical) | | |
| T1 | 272 (51%) | 537 (67.3%) |
| T2 | 69 (13%) | 65 (8.2%) |
| T3 | 180 (34%) | 186 (23.3%) |
| T4 | 11 (2.1%) | 9 (1.1%) |
| Tx | 1 (0.2%) | 0 |
| Lymph nodes status | | |
| N0 | 516 (96.8%) | 787(98.7%) |
| N1+ | 16 (3.0%) | 10 (1.3%) |
| Unknown | 1(0.2%) | 0 |
| Distant metastasis | | |
| M0 | 451 (84.6%) | 797 (100%) |
| M1 | 81 (15.2%) | 0 |
| Unknown | 1 (0.2%) | 0 |
| Fuhrman grade | | |
| 1 | 14 (2.6%) | 143 (17.9%) |
| 2 | 228 (43%) | 395 (49.6%) |
| 3 | 206 (39%) | 171 (21.5%) |
| 4 and/or with sarcomatoid | 76 (14%) | 88 (11.0%) |
| Unknown | 9 (1.7%) | 0 (0%) |
| Coagulative Necrosis | | |
| Absent | 474 (88.9%) | 629 (78.9%) |
| Present | 59 (11.1%) | 168(21.1%) |
| Follow-up duration | | |
| Median (quartile) | 48 (23.0 to 71.0) | 70.0 (64.0 to 72.0) |
| Abbreviation: ccRCC, clear-cell renal cell carcinoma; ECOG-PS, Eastern cooperative Oncology Group performance status; IQR, interquartile range; | | |
| *Outcome estimation was limited to the largest survival time when it is censored; | | |
| †Median follow-up and IQR are reported for patients without the event at end of follow-up. | | |

Supplementary Table 2. Multivariable survival analyses

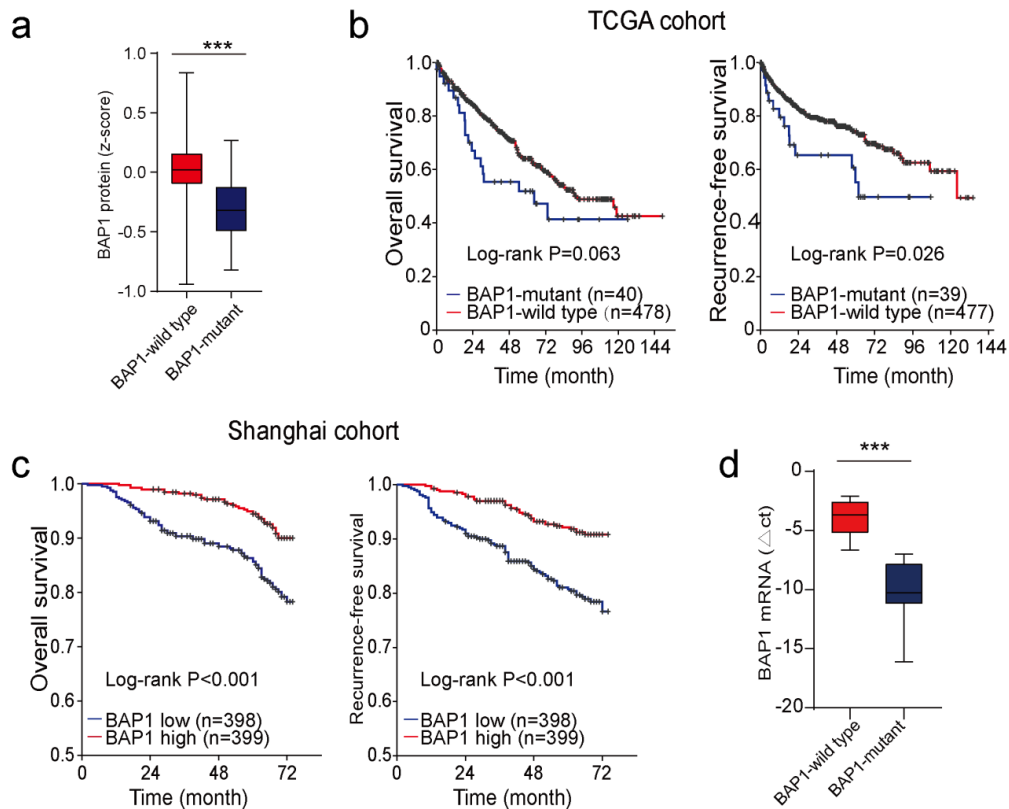
| Variables | TCGA cohort | | Shanghai cohort | |
|---|------------------------|----------|------------------------|----------|
| | HR (95% CI) | <i>P</i> | HR (95% CI) | <i>P</i> |
| OS | | | | |
| Age at surgery (continuous) | 1.033 (1.019 to 1.048) | <0.001 | 1.010 (0.992 to 1.029) | 0.261 |
| Gender (male vs female) | 1.112 (0.801 to 1.543) | 0.526 | 1.722 (1.084 to 2.735) | 0.021 |
| ECOG-PS (≥ 1 vs other) | 0.927 (0.649 to 1.325) | 0.678 | 3.005 (1.937 to 4.662) | <0.001 |
| Tumor size (continuous, cm) | 1.028 (0.985 to 1.072) | 0.205 | 1.385 (1.289 to 1.488) | <0.001 |
| Pathological T stage (pT3+pT4 vs pT1+pT2) | 2.504 (1.782 to 3.519) | <0.001 | 3.238 (2.148 to 4.882) | <0.001 |
| Lymph nodes status (N1 vs Nx+N0) | 1.880 (0.950 to 3.721) | 0.070 | 1.485 (0.957 to 2.303) | 0.078 |
| Necrosis (present vs absent) | 2.601 (1.729 to 3.912) | <0.001 | 3.316 (2.171 to 5.065) | <0.001 |
| BAP1 mRNA expression (high vs low) | 1.389 (0.846 to 2.281) | 0.194 | 1.723 (1.131 to 2.623) | 0.011 |
| RFS | | | | |
| Age at surgery (continuous) | 1.002 (0.986 to 1.018) | 0.820 | 0.998 (0.981 to 1.016) | 0.854 |
| Gender (male vs female) | 1.466 (0.967 to 2.222) | 0.072 | 1.338(0.873 to 2.051) | 0.182 |
| ECOG-PS (≥ 1 vs other) | 0.873 (0.552 to 1.380) | 0.560 | 1.622 (1.035 to 2.545) | 0.035 |
| Tumor size (continuous, cm) | 1.113 (1.066 to 1.161) | <0.001 | 1.401 (1.310 to 1.499) | <0.001 |
| Pathological T stage (pT3+pT4 vs pT1+pT2) | 2.884 (1.931 to 4.309) | <0.001 | 3.394(2.274 to 5.066) | <0.001 |
| Necrosis (present vs absent) | 1.963 (1.195 to 3.223) | 0.008 | 4.128(2.742 to 6.217) | <0.001 |
| BAP1 mRNA expression (high vs low) | 1.724 (0.969 to 3.065) | 0.064 | 1.793 (1.182 to 2.721) | 0.006 |

Abbreviation: HR, Hazard Ratio; CI, confidence interval.



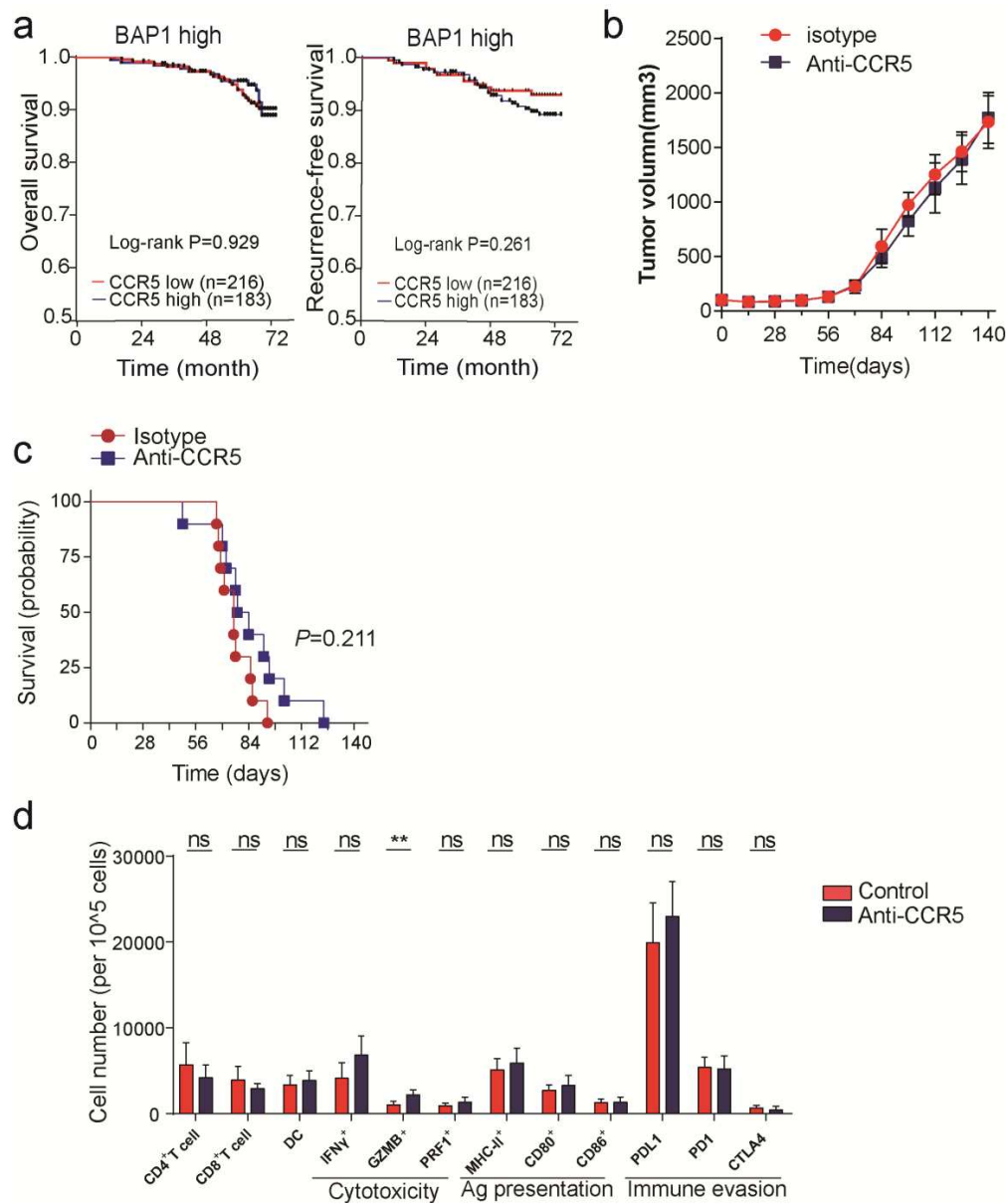
Supplementary Figure 1. Immune characteristics and PD-1 inhibitor treatment among BAP1-mutant ccRCC patients from previous study

(a) Immune characteristics of BAP1 mutant ccRCC based on the TCGA database. Box-and-whisker diagrams were used (median, lower, and upper quartiles; horizontal lines define Min and max). (b-c) BAP1 mutant ccRCC patients have poor clinical response to immune checkpoint PD-1 inhibitor treatment. CB = clinical benefit; IB =intermediate benefit; NCB = no clinical benefit. Without statistical difference due to the small scale of cohorts.



Supplementary Figure 2. BAP1 gene mutation is associated with poor prognosis in ccRCC patients

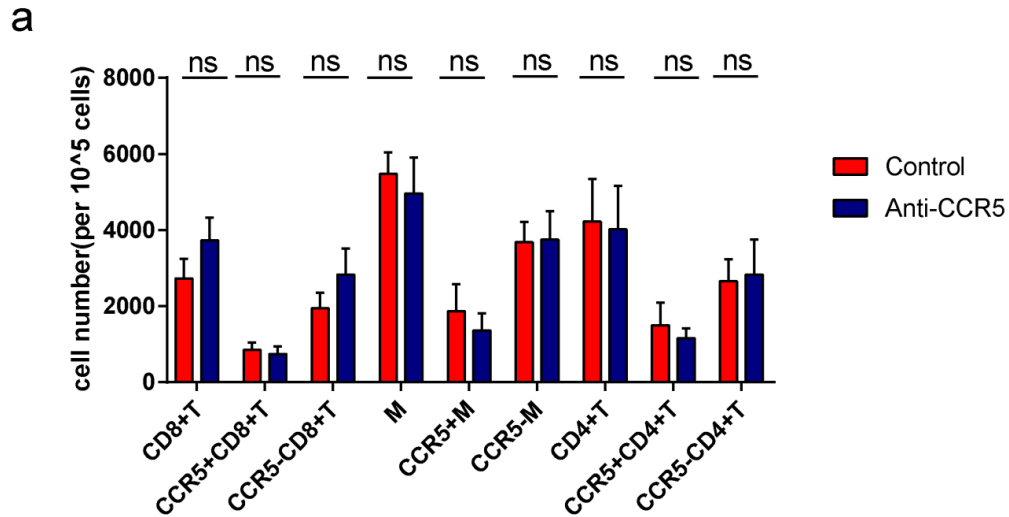
(a) Expression of BAP1 protein (normalized as Z-score) in BAP1-mutant and BAP1-wildtype ccRCC patients. Box-and-whisker diagrams were used (median, lower, and upper quartiles; horizontal lines define Min and max). (b) OS ($n = 518$) and RFS ($n = 516$) curves of ccRCC patients from the TCGA cohort according to the BAP1 mRNA level. (c) OS and RFS curves of ccRCC patients from a shanghai cohort according immunohistochemical CCR5 staining intensity ($n = 797$). (d) BAP1-wild type ($n = 8$) and BAP1-mutant ($n = 8$) patients defined by BAP1 mRNA level.



Supplementary Figure 3. Blockade of CCR5 has no significant therapeutic effect in a ccRCC tumor mouse model with normal BAP1 gene expression

(a) OS and RFS curves for BAP1-high ccRCC patients according to immunohistochemical CCR5 staining intensity from shanghai cohort. (b) Tumor volume from BALB/c mice subcutaneously injected with BAP1-wildtype RENCA cells and treated with anti-CCR5 or

isotype ($n = 10$ per group). (c) OS curve for BALB/c mice orthotopically injected with RENCA cells and treated with anti-CCR5 or isotype antibodies ($n = 10$ per group). (d) Number of intratumoral CD4⁺ T cells, CD8⁺ T cells, DC, IFN- γ ⁺, GZMB⁺, PRF1⁺, CD80⁺, CD86⁺, MHC-II⁺, PD-L1⁺, PD-1⁺, CTLA-4⁺ cells from BALB/c mice orthotopically injected with RENCA cells and treated with anti-CCR5 or isotype antibodies ($n = 10$ per group).

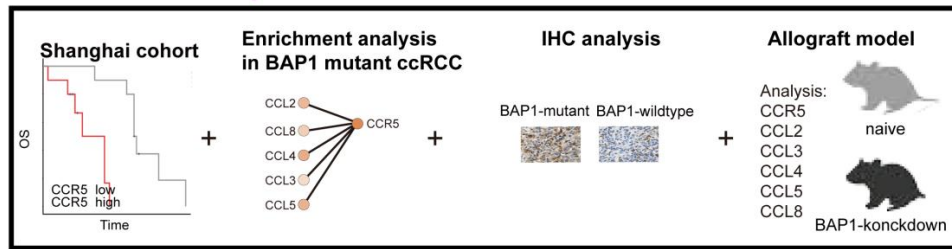


Supplementary Figure 4. Changes in the tumor-infiltrating immune cells after blockade of CCR5 in a BAP1-knockdown ccRCC tumor mouse model.

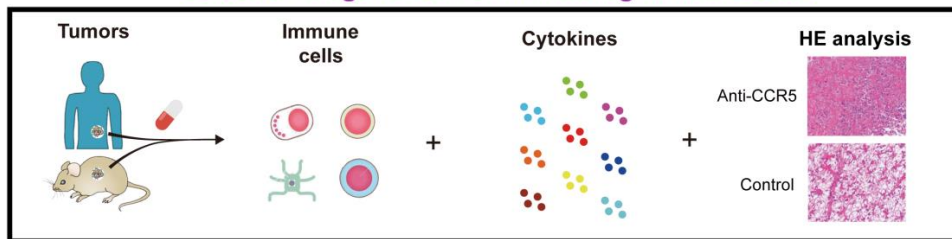
(a) Number of intratumoral CD8⁺ T cells, conventional CD4⁺ T cells, macrophages and CCR5⁺ or CCR5⁻ subpopulations correspondingly from BALB/c mice subcutaneously injected with BAP1-knockdown RENCA cells and treated with anti-CCR5 or isotype antibodies ($n = 5$ per group). M = macrophages

Graphic abstract

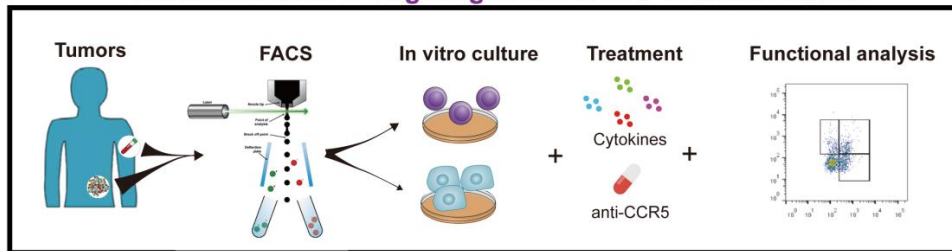
Expression of CCR5 in BAP1 mutant ccRCC



Effect of drugs on tumor infiltrating immune cells



The mechanism of targeting CCR5 in BAP1 mutant ccRCC



Blocking CCR5 has therapeutic effect on BAP1 mutant ccRCC

